Journal of
Materials Chemistry B

ROYAL SOCIETY OF CHEMISTRY

PAPER

View Article Online
View Journal

Cite this: DOI: 10.1039/c4tb00607k

Magnetic molecularly imprinted polymers (MMIPs) for carbazole derivative release in targeted cancer therapy†

Ortensia Ilaria Parisi,[ab] Catia Morelli,[a] Francesco Puoci,*[a] Carmela Saturnino,[c] Anna Caruso,[ab] Diego Sisci,[a] Giovanna Elvi Trombino,[a] Nevio Picci[a] and Maria Stefania Sinicropi[a]

Received 16th April 2014
Accepted 6th August 2014

DOI: 10.1039/c4tb00607k

www.rsc.org/MaterialsB

The synthesis of an innovative delivery system for targeted cancer therapy which combines the drug controlled release ability of Molecularly Imprinted Polymers (MIPs) with magnetic properties of magnetite is described herein. In the present study, an easy and smart synthetic strategy, involving new engineered precipitation photo-polymerization, was developed with the aim to obtain Magnetic Molecularly Imprinted Polymers (MMIPs) for 9*H*-carbazole derivative sustained delivery in cancer treatment. Both *in vitro* drug release and cytotoxicity studies on different cancer cell lines, such as HeLa and MCF-7, were performed in order to evaluate the controlled release ability and the potential application as a drug carrier in targeted cancer therapy. The synthesized polymeric materials have shown not only good selective recognition and controlled release properties, but also high magnetic responding capacity. The performed cytotoxicity studies highlighted the high inhibitory activity against the tested cell lines due to a dramatic growth arrest, compared to controls, by triggering apoptosis. These results clearly indicate the potential application of synthesized MMIPs as a magnetic targeted drug delivery nanodevice.

1. Introduction

Conventional cancer chemotherapy presents relevant limitations associated with the non-selectivity of cytotoxic drugs, their narrow therapeutic indices and limited cellular penetration. Anticancer agents, indeed, are not able to discriminate between cancerous and healthy cells and tissues as well, leading to severe systemic toxicity and undesired side effects. Over the last few decades, indeed, the research interest was focused on the development of novel materials based on different components, including proteins, metals, lipids, polymers and dendrimers, with the aim to prepare suitable drug delivery platforms to be employed in anticancer therapy.[1–3]

A possible approach to overcome these drawbacks is the development of innovative therapeutic strategies involving the use of tumor-targeted delivery systems able to promote specific drug accumulation at the pathological site. An ideal delivery vehicle has to ensure not only that the therapeutic agent is released at the right site, but also in the right dose and for the required period of time in order to maximize its efficiency.

Based on these considerations, the aim of the present study was to prepare an innovative delivery nanodevice for targeted cancer therapy by combining the drug controlled release ability of Molecularly Imprinted Polymers (MIPs) with magnetic properties of magnetite.

Molecular imprinting represents a very promising and attractive technology for the synthesis of polymeric matrices characterized by specific recognition capabilities for a desired template molecule.[4] The specific recognition properties of imprinted polymers are due to the formation of a complex between the template and functional monomers during the pre-polymerization step. For this purpose, the chosen monomers have to exhibit chemical structures able to interact with the template molecule in a covalent or non-covalent way. After the formation of the pre-polymerization complex, monomers are polymerized in the presence of a crosslinking agent and, subsequently, the template is removed by washing and/or solvent extraction. The obtained imprinted polymer presents binding sites, which are complementary in size, shape and functional groups to the template, and it is able to re-bind the analyte of interest with high selectivity.

Due to their high stability against chemical and enzymatic attack, high selectivity for a specific template, low cost and easy preparation, MIPs could find applications in a wide range of fields such as preparative and analytical separation, solid-phase

[a]Department of Pharmacy, Health and Nutritional Sciences, University of Calabria, 87036 Rende, CS, Italy. E-mail: francesco.puoci@unical.it; Tel: +39 (0)984 493151

[b]Department of Informatics, Modeling, Electronics and Systems Engineering, University of Calabria, 87036 Rende, CS, Italy

[c]Department of Pharmaceutical and Biomedical Sciences, University of Salerno, 84084 Fisciano, SA, Italy

† Electronic supplementary information (ESI) available. See DOI: 10.1039/c4tb00607k

Published on 07 August 2014. Downloaded by University of Calabria on 03/09/2014 18:12:45.

Published on 07 August 2014. Downloaded by University of Calabria on 03/09/2014 18:12:45.

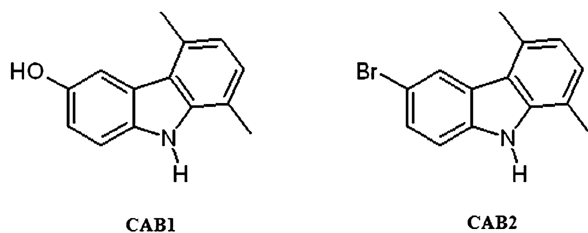

Fig. 1 Chemical structures of CAB1 and CAB2.

extraction, antibody and enzyme mimics, biosensors and synthetic receptors for proteins and biological molecules.[5–9]

During the last few years, the potential application of MIPs in drug delivery has received considerable attention. These systems can regulate drug release by increasing the residence time of the therapeutic agent within the polymeric matrix, by means of either covalent or non-covalent interactions in specific binding sites. This results in a reduced rate at which the drug is released from the polymeric material. Thus, the application of MIPs as base excipients for the controlled release of drugs characterized by a narrow therapeutic index could avoid adverse side effects due to an over-concentration of the therapeutic compound.

Until now, few publications[10,11] report on the preparation of Magnetic Molecularly Imprinted Polymers (MMIPs) for drug delivery synthesized by thermo-induced polymerization while, in the present study, an easy and smart synthetic strategy, involving new engineered precipitation photo-polymerization, was developed with the aim to obtain MMIPs for 9*H*-carbazole derivative sustained delivery in targeted cancer therapy.

Many of these compounds, indeed, have shown cytotoxic and anti-neoplastic properties, even if their specific mechanism of action has not yet been explained. It was suggested that the intercalation of these molecules into DNA and the inhibition of the DNA-topoisomerase II activity are the basis of the antitumor and cytotoxic effects.[12,13] In this regard, 1,4-dimethyl-6-hydroxy-9*H*-carbazole (CAB1, Fig. 1) was chosen as a template molecule due to its high cytotoxic activity and significant ability to inhibit proliferation of different cancer cell lines such as MCF-7.[14]

Synthesized magnetic imprinted nanospheres could be employed to deliver the anti-neoplastic agent to the desired tumor area by the application of an external localized magnetic field while the spherical shape provides an isotropic release behaviour.[15] Furthermore, it is well known that the permeation ability of nanoparticles results in an enhanced cellular uptake of the therapeutic agent. In this way, it is possible to obtain a delivery system able to release the drug with both a spatial and a temporal control.

2. Experimental

2.1 Materials, cell lines and culture conditions

Methacrylic acid (MAA), ethylene glycol dimethacrylate (EGDMA), 2,2′-azoisobutyronitrile (AIBN), disodium hydrogen phosphate, sodium dihydrogen phosphate, iron(II) chloride tetrahydrate ($FeCl_2 \cdot 4H_2O$), iron(III) chloride hexahydrate ($FeCl_3 \cdot 6H_2O$), sodium hydroxide (NaOH), bovine serum albumin (BSA) were purchased from Sigma-Aldrich (Sigma Chemical Co., St Louis, MO, USA).

MAA and AIBN were purified before use by distillation under reduced pressure and recrystallization from methanol, respectively.

The template 1,4-dimethyl-6-hydroxy-9*H*-carbazole (CAB1) and its analogue 6-bromo-1,4-dimethyl-9*H*-carbazole (CAB2, Fig. 1) were synthesized as reported elsewhere[12] and provided by the Laboratory of Pharmaceutical and Toxicological Chemistry, Department of Pharmacy, Health and Nutritional Sciences, University of Calabria (Italy).

All solvents were of reagent grade or HPLC-grade and provided by Carlo Erba reagents (Milan, Italy).

HeLa cervical adenocarcinoma cells and MCF-7 breast cancer cells were purchased from Interlab Cell Line Collection, ICLC, Genoa, Italy. HeLa and MCF-7 were grown in modified Eagle's medium (MEM, Sigma-Aìdrich, Milan, Italy) plus 10% fetal bovine serum (FBS) and Dulbecco's modified Eagle's/Ham's F-12 medium (1 : 1) (DMEM-F12) plus 5% FBS, respectively. Culture media were supplemented with 100 IU mL^{-1} penicillin, 100 mg mL^{-1} streptomycin, and 0.2 mM L-glutamine (all from Life Technologies, Monza, Italy). Cells were maintained as monolayer culture in a humidified incubator at 5% CO_2 and 37 °C.

2.2 Instrumentation

UV-Vis absorption spectra were obtained with a Jasco V-530 UV/Vis spectrometer.

IR spectra were recorded with films or KBr pellets using a Jasco FT-IR 4200.

The scanning electron microscopy (SEM) photographs were obtained with a Jeol JSMT 300 A; the surface of the samples was made conductive by deposition of a gold layer on the samples in a vacuum chamber. An approximate range in the particle size was determined employing an image processing and analysis system, a Leica DMRB equipped with a LEICA Wild 3D stereomicroscope.

Sample magnetization was measured as a function of the applied magnetic field *H* with a 9600 VSM (LDJ, USA) superconducting quantum interference device (SQUID) magnetometer. The hysteresis of magnetization was obtained by changing *H* between +20 000 and −20 000 Oe at room temperature.

2.3 Preparation of magnetite (Fe_3O_4)

Fe_3O_4 particles were prepared according to the co-precipitation method.[16]

Initially, 0.01 mol of $FeCl_2 \cdot 4H_2O$ and 0.02 mol of $FeCl_3 \cdot 6H_2O$ were dissolved in 100 mL of water. The mixture was stirred vigorously and purged with a nitrogen gas while the temperature increased to 80 °C, and then 40 mL of sodium hydroxide solution (2 M) was added into it. After 1 h and completion of the reaction, the black magnetic precipitate was collected by an external magnetic field and washed several times with water and ethanol, and finally dried under vacuum.

 This journal is © The Royal Society of Chemistry 2014

Published on 07 August 2014. Downloaded by University of Calabria on 03/09/2014 18:12:45.

2.4 Synthesis of Magnetic Molecularly Imprinted Polymers (MMIPs)

Magnetic molecularly imprinted nanospheres were prepared by precipitation polymerization following the reported procedure.

Briefly, 1 mmol of template CAB1 and 8 mmol of functional monomer MAA were dissolved in a mixture of acetonitrile (20 mL) and toluene (20 mL), in a 100 mL round bottom flask and sonicated for 10 min in order to form a template–monomer complex. Then, 10 mmol of EGDMA, 0.5 g of magnetite and 100 mg of AIBN were added and the mixture was purged with nitrogen and sonicated for 10 min. The flask was gently agitated (40 rpm) and then the mixture was photo-polymerized for 24 h with 360 nm light at 4 °C. At the end of the reaction, the particles were filtered, washed with 100 mL of ethanol, 100 mL of acetone, and then with 100 mL of diethyl ether. The template was extracted by a "Soxhlet apparatus" using 200 mL of an acetic acid–methanol (1 : 9, v/v) mixture for at least 48 h, followed by 200 mL of methanol for another 48 h. Particles were successively dried under vacuum overnight at 40 °C.

MMIP materials were checked to be free of CAB1 and any other compound by UV-Vis analysis.

For comparison, magnetic non-molecularly imprinted polymers (MNIPs) were also prepared in the absence of CAB1 during the polymerization process and treated under the same conditions.

2.5 Binding experiments: the imprinting effect and selectivity properties

Binding experiments were carried out in order to evaluate the recognition properties and the selectivity of MMIP materials.

For this purpose, 100 mg of polymeric nanospheres were mixed with 3 mL of CAB1 standard solution (0.1 mM) in EtOH–H_2O (1 : 1, v/v). Samples were shaken in a water bath at 37 ± 0.5 °C for 24 h, centrifuged for 10 min (6000 rpm) and the concentration of free CAB1 in the liquid phase was measured by UV-Vis spectrometry.

A calibration curve was recorded by using five different CAB1 standard solutions and the correlation coefficient (R^2), slope and intercept of the regression equation were obtained by the method of least square.

With the aim to evaluate the selectivity of MMIPs, the same binding experiments were performed using CAB2 solutions.

All the experiments were repeated three times.

2.6 Protein adsorption measurement

BSA was dissolved in a 25 mM phosphate buffer solution at pH 7.4.

In each experiment, 150 mg of MMIP and MNIP nanospheres were packed into 6.0 mL polypropylene SPE columns. The columns were attached with a stop cock and a reservoir at the bottom end and the top end, respectively. Before use, the columns were preconditioned by successive washing steps with water, HCl (0.07 M), water, MeOH–water (50 : 50, v/v), water, and finally 25 mM phosphate buffer (pH 7.4). The adsorption test was performed by loading the cartridges with 2.0 mL of the prepared BSA standard solution (1.2 mg mL^{-1}).[17]

The amount of adsorbed protein after the loading step was calculated by using a UV-Vis spectrophotometer at 290 nm.

Experiments were repeated three times.

2.7 Swelling behaviour

Aliquots (50 mg) of the nanospheres dried to a constant weight were placed in a tared 5 mL sintered glass filter (Ø 10 mm; porosity, G3), weighed, and left to swell by immersing the filter plus support in a beaker containing phosphate buffer (pH 7.4, simulated biological fluids) as the swelling media. At the predetermined time (24 h), the excess water was removed by percolation at atmospheric pressure. Then, the filter was placed in a properly sized centrifuge test tube by fixing it with the help of a bored silicone stopper, and then centrifuged at 3500 rpm for 15 min and weighed. The filter tare was determined after centrifugation with only water. The weight recorded was used to give the water content percentage (WR%) by the following eqn (1):

$$\mathrm{WR\%} = \frac{W_\mathrm{s} - W_\mathrm{d}}{W_\mathrm{d}} \times 100 \quad (1)$$

where W_s and W_d are weights of swollen and dried spherical nanoparticles, respectively.

Each experiment was carried out in triplicate.

2.8 Drug loading by the soaking procedure

100 mg of polymeric nanospheres were immersed in 1.5 mL of CAB1 solution (16 mM) in ethanol and soaked for 3 days at room temperature. During this time, the mixture was continuously stirred, and then the solvent was removed under reduced pressure.

2.9 *In vitro* release studies

In vitro release studies were carried out using the dissolution method described in the USP XXIV (apparatus 1 basket stirring element).

An amount of MMIP and MNIP nanospheres (10 mg) loaded with CAB1 was dispersed in flasks containing 10 mL of PBS (0.01 M) at pH 7.4 and maintained at 37 ± 0.5 °C in a water bath with stirring (50 rpm). These conditions were maintained throughout the experiment.

In order to characterize the drug release, 3 mL of samples were drawn from the dissolution medium at designated time intervals, and the same volume of simulated fluid was supplemented. CAB1 was determined by UV-Vis analyses and the percentage of the released drug was calculated considering 100% of the CAB1 content in polymeric samples after the drying procedure.

Experiments were repeated three times and the results were expressed as means (±SEM).

Published on 07 August 2014. Downloaded by University of Calabria on 03/09/2014 18:12:45.

2.10 Cell viability

The effect of MMIP nanospheres loaded with CAB1 (MMIPs-CAB1) on cell proliferation was assessed by trypan blue exclusion assay.

HeLa cells were plated in triplicates in 12-well plates at a concentration of 5×10^4 cells per well and grown overnight. Next day, cells were shifted in serum free media (SFM) for 24 h to synchronize the cells in the same cell cycle phase, thus avoiding growth differences among cells. Following starvation, 50 μg per well of MMIP-CAB1, corresponding to a concentration of about 10 μM CAB1, were resuspended in 1% FBS growing medium and added to the cells. As negative controls, the vehicle alone (DMSO) or MMIPs were added to the cells in the same amount used for MMIP-CAB1. After 1, 2 or 3 days, cells were harvested by trypsinization and incubated in a 0.5% trypan blue solution for 10 min at room temperature. The cell viability was determined microscopically by counting trypan blue negative cells in a hemacytometer (Burker, Brand, Germany).

2.11 TUNEL assay

Apoptosis was determined as previously described[18] by enzymatic labeling of DNA strand breaks by terminal deoxynucleotidyl transferase-mediated deoxyuridine triphosphate nick-end labeling (TUNEL), using a Dead End Fluorometric TUNEL System (Promega, Italy) according to the manufacturer's instructions. 3×10^5 HeLa cells were seeded on coverslips in 35 mm Petri dishes and then treated as described for growth experiments. After 72 hours of incubation, coverslips were mounted on slides using Fluoromount mounting medium (Sigma-Aldrich, Italy) and observed under a fluorescence microscope (Olympus BX51, Olympus Italia srl, Milan, Italy). 4′,6-Diamidino-2-phenylindole (DAPI, Sigma-Aldrich, Italy) was used to counterstain the nuclei. Apoptotic cells were photographed at 10× magnification using ViewFinder™ 7.4.3 Software, through an Olympus camera system dp50 and then counted using Image J software (NIH, USA).

3. Results and discussion

3.1 Synthesis and characterization of MMIPs

Magnetic nanospheres imprinted for the anti-neoplastic drug CAB1 were synthesized by precipitation photo-polymerization following the non-covalent approach.

Although bulk polymerization is widely employed in order to prepare MIP materials, this technique presents some disadvantages such as the possibility to destroy imprinted cavities during the grinding step. On the other hand, precipitation polymerization is a heterogeneous polymerization technique which allows obtaining clean and uniform particles, characterized by the regular size and shape, without any further treatment and in the absence of any surfactant.

In precipitation polymerization, the polymerization system consists of only the functional monomer, cross-linker, initiator and solvent as components[19] and, in the first stage of the reaction process, monomers form oligomer radicals. Then, the formed oligomers crosslink and the obtained crosslinked nuclei aggregate into larger particles leading to the formation of the final polymer beads. The number of particles is determined by this first stage of the process and then remains constant, only the size grows in the later stages.[20] Several factors affect the particle size, morphology and size distribution including the adopted concentrations of the monomer, cross-linking agent and initiator. The diameter of polymeric spheres, indeed, increases with increasing monomer or initiator concentration;[21] on the other hand, the particle size decreases as the cross-linker percentage increases.[22] Furthermore, the increasing initiator concentration would accelerate the reaction rate resulting in faster growth of the particles.

In the present study, the developed synthetic strategy allowed the preparation of magnetic imprinted nanospheres without the use of dispersants, such as polyvinylpyrrolidone, and performing the reaction at low temperature which is important to avoid drug degradation. In the prepolymerization feed the employed MAA/EGDMA molar ratio was equal to 8 : 10. This ratio allowed obtaining polymeric particles characterized by the desired properties, such as the spherical shape and nanometer size. Nanomaterials, indeed, are able to overcome cellular penetration constraints. Spherical geometry and the practical monodispersion of the prepared nanospheres were, indeed, confirmed by scanning electron micrographs (Fig. 2).

Natural recognition is driven largely by non-covalent forces, such as ionic interactions, hydrogen bonding, and van der Waals forces, and thus, the non-covalent approach is preferred to the covalent one in biological applications. In this method, non-covalent forces are involved in both the pre-polymerization process and the rebinding step. Although non-covalent interactions are relatively weak, they allow binding of their targets with exceptionally strong affinities. Moreover, this strategy is characterized by fast kinetics of binding and the absence of toxic reaction products, and a wide range of functional monomers, acidic, basic or neutral, can be used for imprinted polymer synthesis.

The incorporation of magnetite was evaluated by performing FT-IR analyses and FT-IR spectra of Fe_3O_4, magnetic MIP and pure MIP particles (synthesized in the absence of magnetite) are compared in Fig. 3.

In Fe_3O_4 spectrum, the peak at 582 cm^{-1} is characteristic of the Fe–O bond. The incorporation of magnetite into the MMIP sample was confirmed by the appearance of a band at 590 cm^{-1}, ascribable to the Fe–O bond, which is absent in the pure MIP particle spectrum.

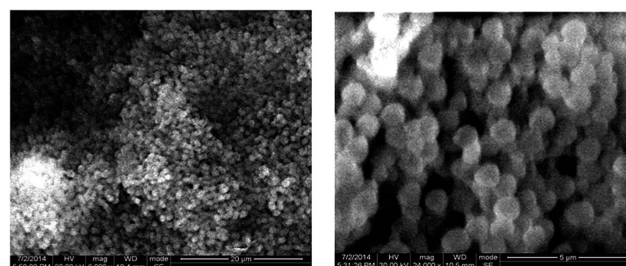

Fig. 2 Scanning electron micrographs of MMIP nanospheres.

This journal is © The Royal Society of Chemistry 2014

Published on 07 August 2014. Downloaded by University of Calabria on 03/09/2014 18:12:45.

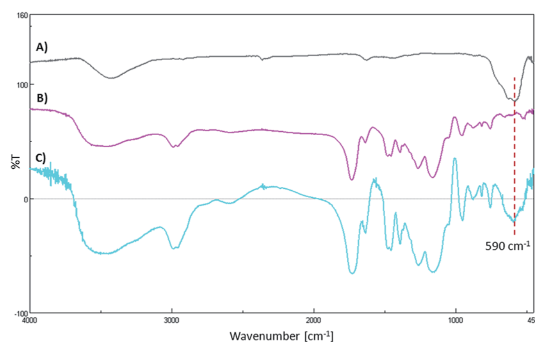

Fig. 3 FT-IR spectra of magnetite (A), pure MIP particles synthesized in the absence of magnetite (B) and magnetic MIP (C).

The magnetic properties of the synthesized MMIP particles were studied by recording magnetization (M) values against the applied magnetic field (H) at 300 K using a VSM. The magnetization hysteresis loops of Fe_3O_4 and MMIPs and a dispersion photograph of magnetic nanospheres in water are shown in Fig. 4. The obtained hysteresis loops and the separation of the nanoparticles by using a magnet confirmed the magnetic behavior of the polymeric material.

This phenomenon is attributable to the presence of magnetite and it is considered to be of relevant interest for targeted drug delivery.

3.2 Imprinting effect and selectivity properties of MMIP particles

The imprinting effect of magnetic MIPs was evaluated by binding experiments in which amounts of polymeric nanospheres were incubated with a CAB1 standard solution (0.1 mM) for 24 hours.

Magnetic MIPs have shown higher adsorption capacity than MNIPs due to the presence of specific binding cavities for CAB1 (Table 1), although these two polymeric materials are composed of exactly the same composition.

The selectivity tests were carried out under equilibrium binding conditions using a molecule structurally similar to the template, such as 6-bromo-1,4-dimethyl-9H-carbazole (CAB2). The chemical differences between the two

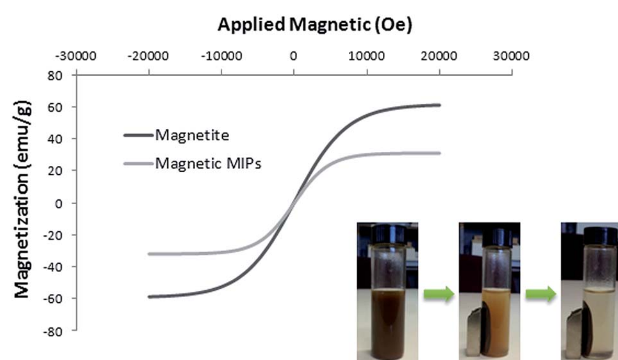

Fig. 4 Magnetization hysteresis loops.

Table 1 Percentages of bound CAB1 and CAB2 by im-printed and non-imprinted nanospheres. Data are shown as mean ± S.D.

Bound CAB1 (%)		Bound CAB2 (%)	
MMIP	MNIP	MMIP	MNIP
52 ± 0.3	38 ± 0.2	79 ± 0.1	76 ± 0.5

compounds, the template CAB1 and its analogue CAB2, drive the interactions with the synthesized polymeric matrices. The selective interaction between the polymeric matrices and the template is, indeed, ascribable to the hydroxyl group of CAB1. The amount of CAB2 bound by the imprinted and the non-imprinted nanospheres was practically the same (Table 1), and this result confirmed the non-specific nature of these interactions.

The imprinting efficiency (α) represents the easiest way to highlight the recognition properties of imprinted materials and it is defined as the ratio of adsorption percentages obtained between the MMIPs and MNIPs. In the present study, the imprinting efficiency was evaluated for each analyte by the following eqn (2):

$$\alpha = \%\text{MMIP}/\%\text{MNIP} \quad (2)$$

The obtained α values for CAB1 and CAB2 were 1.4 and 1.0, respectively.

The selectivity of the synthesized magnetic nanospheres can be highlighted by introducing another coefficient (ε), which is calculated as the ratio between the amounts (%) of CAB1 and CAB2 bound by MMIPs. This value was found to be equal to 0.7.

These results indicated that the imprinted magnetic nanospheres exhibited higher binding capacity and selectivity for CAB1 than the corresponding non-imprinted material indicating the specificity of the interaction between the template and the functional groups on the polymeric nanospheres. The imprinting process, indeed, allows the formation of binding sites into the polymeric matrix characterized by the shape and the functional group complementary to the template molecule.

3.3 Protein adsorption measurement and swelling behavior

The hydrophilic properties of the prepared magnetic nanospheres play a key role in determining the unspecific protein adsorption and the swelling properties in water media of these polymeric systems affecting their biocompatibility.

The unspecific adsorption of proteins on the MMIP nanosphere surface has to be avoided because it could interfere with the interactions with smaller molecules such as the template.

In this study, BSA was employed as a model protein with the aim to evaluate the non-specific hydrophobic adsorption level of the synthesized magnetic nanospheres. The observed BSA binding capacity of the synthesized polymeric materials is

Published on 07 August 2014. Downloaded by University of Calabria on 03/09/2014 18:12:45.

Table 2 Hydrophilic properties of polymeric nanospheres: water content (%) and percentage of bound BSA. Data are shown as mean ± S.D.

Polymer	Water content (%)	Bound BSA (%)
MMIP	374 ± 0.3	15 ± 0.2
MNIP	369 ± 0.4	19 ± 0.1

reported in Table 2 confirming a low level of unspecific adsorption which is required in biological applications.

In order to evaluate the swelling properties of MMIPs and MNIPs, aliquots of nanospheres were immersed in a phosphate buffer solution at pH 7.4, simulating the biological fluids. The obtained results (Table 2) indicated good swelling characteristics which make the imprinted cavities easily accessible to the template improving recognition properties.

3.4 *In vitro* release studies

After the evaluation of the adsorption and selectivity properties of magnetic MIPs, the controlled release capacity of the template molecule in plasma simulating fluids was verified.

Fig. 5 shows the *in vitro* release profile of CAB1 from imprinted and non-imprinted nanospheres at 37 °C and, as it is possible to note, about 19% of the total loaded CAB1 was released during the first hour from the imprinted matrix, while MNIPs released about 49% within the same time.

The therapeutic agent was, indeed, completely released within 6 hours by MNIPs, while for MMIP samples even after 48 h the drug release was not complete. CAB1 adsorption onto MNIPs during the loading step was mainly due to unspecific interactions and physical adsorption onto the nanospheres' surface by weak interactions; this explains why the drug was released in a shorter time period from the non-imprinted matrix.

On the other hand, the more extended overtime CAB1 release observed with MMIPs could be ascribable to the presence of deeper and imprinted cavities inside the polymeric matrix. The aqueous medium access to the binding sites, indeed, needs long time for diffusion and template molecules were bound more strongly to the MMIP matrix.

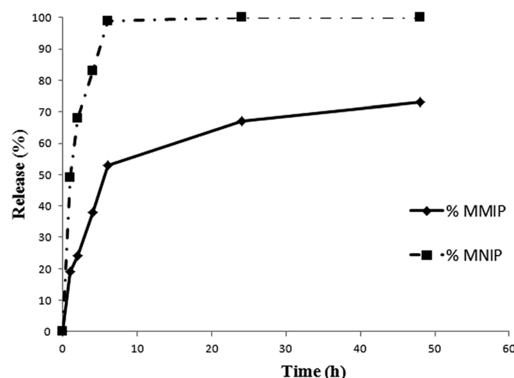

Fig. 5 Release profile of CAB1 in a buffer solution at pH 7.4.

MMIPs have shown controlled release capacity of the therapeutic agent and the rate of CAB1 release from imprinted and non-imprinted materials was considerably different.

3.5 Cytotoxicity studies against cancer cells

Viability experiments were conducted on HeLa and MCF-7 cancer cells with the aim to investigate the potential application of the magnetic imprinted nanospheres as a drug carrier in targeted cancer therapy.

In HeLa cells, a strong growth retardation, was observed after 2 and 3 days of exposure to MMIP-CAB1, if compared to the relative controls (DMSO) (Fig. 6A). The effect was even more evident in MCF-7 cells, which, with respect to DMSO treated cells, showed a dramatic growth retardation already after one day of MMIP-CAB1 treatment, reaching an almost complete growth inhibition on day 3 (Fig. 6B).

It is worthy to underline that, in HeLa cells, polymers (MMIPs) alone did not show any significant effect at all-time points tested if compared to a control vehicle (DMSO), while a slight, although not significant, toxicity could be detected in MCF-7 cells (Fig. 6A and B).

These results confirm previously published data reporting no detectable MIP toxicity, both on cell systems[23] and in mouse models.[24]

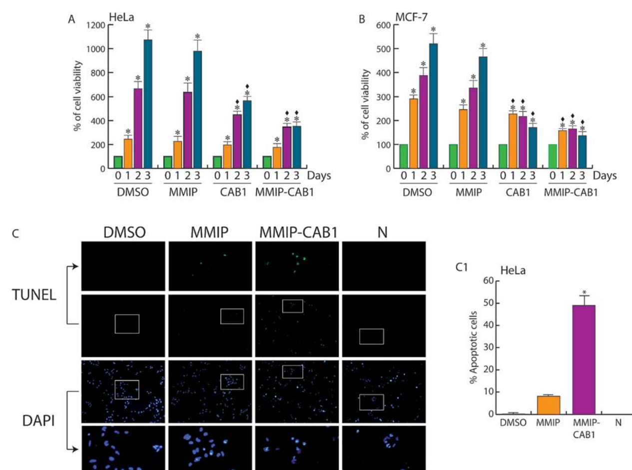

Fig. 6 *In vitro* cytotoxicity studies. MMIP nanospheres loaded with CAB1 (MMIP-CAB1) retain the ability of inducing death in cancer cells. HeLa (A) and MCF-7 (B) cells were treated with DMSO (used as control), polymer alone (MMIP) or MMIP-CAB1. The viability was determined as described in Materials and methods after 1, 2 and 3 days. Values represent the mean of four triplicate independent experiments and are reported as % of cell viability. The error bars indicate SD. *p < 0.0l *vs.* day 0; ◆p < 0.01 *vs.* the respective days in DMSO. (C) HeLa cells, treated as above, were subjected to TUNEL assay and observed under a fluorescent microscope (see Materials and methods). An additional MMIP-CAB1 treated sample was exposed to the reaction mixture lacking the enzyme solution and used as a negative control (*N*). The blue dye DAPI was used to counterstain nuclei. Images were taken at 10× magnification, and enlarged images of representative areas are reported as well. (C1) Apoptotic cells and stained nuclei were counted using Image J software. Histograms represent the apoptotic index (% apoptotic cells per total nuclei in the field). *P < 0.01 *vs.* DMSO and MMIP samples.

 This journal is © The Royal Society of Chemistry 2014

Published on 07 August 2014. Downloaded by University of Calabria on 03/09/2014 18:12:45.

Tunel assay further corroborated MMIP biocompatibility, as evidenced by the presence of very few (~7%) apoptotic cells in MMIP treated samples. In contrast, the same amount of MMIP-CAB1 was able to induce apoptosis in about 50% of treated cells (Fig. 6C and C1).

This observation suggests that the growth arrest of MMIP-CAB1 treated cells, might be, most likely, due to a later apoptotic event rather than an early inhibition of proliferative pathways.

4. Conclusions

The present study describes the synthesis of an innovative delivery nanodevice for targeted cancer therapy which combines the drug controlled release ability of Molecularly Imprinted polymers with magnetic properties of magnetite. MMIPs were synthesized by precipitation photo-polymerization of methacrylic acid and ethylene glycol dimethacrylate around the template molecule and in the presence of magnetite.

The synthesized polymeric materials have shown not only good selective recognition and controlled release properties, but also high magnetic responding capacity. Furthermore, the performed cytotoxicity studies highlighted the high inhibitory activity against HeLa and MCF-7 cancer cell lines due to a dramatic growth arrest, compared to controls, by triggering apoptosis.

These results clearly indicated the potential application of the prepared imprinted nanospheres in targeted cancer therapy.

Acknowledgements

The financial support of the Italian Minister of University and Research and University of Calabria is most gratefully acknowledged.

Notes and references

1 B. Y. Kim, J. T. Rutka and W. C. Chan, *N. Engl. J. Med.*, 2010, **363**, 2434–2443.
2 K. H. Bae, H. J. Chung and T. G. Park, *Mol. Cells*, 2011, **31**, 295–302.
3 A. Taylor, K. M. Wilson, P. Murray, D. G. Fernig and R. Levy, *Chem. Soc. Rev.*, 2012, **41**, 2707–2717.
4 D. R. Kryscio and N. A. Peppas, *Acta Biomater.*, 2012, **8**, 461–473.
5 T. Hishiya, H. Asanuma and M. Komiyama, *Polym. J.*, 2003, **35**, 440–445.
6 J. O. Mahony, K. Nolan, M. R. Smyth and B. Mizaikoff, *Anal. Chim. Acta*, 2005, **534**, 31–39.
7 B. Sellergren and C. Alexander, *Adv. Drug Delivery Rev.*, 2005, **57**, 1733–1741.
8 S. Wei, M. Jakusch and B. Mizaikoff, *Anal. Chim. Acta*, 2006, **578**, 50–58.
9 T. S. Anirudhan and S. Sandeep, *Polym. Chem.*, 2011, **2**, 2052–2061.
10 X. Kan, Z. Geng, Y. Zhao, Z. Wang and J. Zhu, *J. Nanotechnol.*, 2009, **20**, 165601–165607.
11 P. Dramou, P. Zuo, H. He, L. A. Pham-Huy, W. Zou, D. Xiao, C. Pham-Huy and T. Ndorbor, *J. Mater. Chem. B*, 2013, **1**, 4099–4109.
12 (*a*) C. Auclair, *Arch. Biochem. Biophys.*, 1987, **259**, 1–14; (*b*) A. Panno, M. S. Sinicropi, A. Caruso, H. El-Kashef, J. C. Lancelot, G. Aubert, A. Lesnard, T. Cresteil and S. Rault, *J. Heterocycl. Chem.*, 2013, DOI: 10.1002/jhet.1951; (*c*) J. Sopkovà-de Oliveira Santos, A. Caruso, J. F. Lohier, J. C. Lancelot and S. Rault, *Acta Crystallogr.*, 2008, **C64**, o453–o455; (*d*) J. F. Lohier, A. Caruso, J. Sopkovà-de Oliveira Santos, J. C. Lancelot and S. Rault, *Acta Crystallogr., Sect. E: Struct. Rep. Online*, 2010, **66**, o1971.
13 (*a*) M. Stiborova, M. Rupertova, H. H. Schmeiser and E. Frei, *Bio-med. Pap. Med. Fac. Univ. Palacky Olomouc Czech Repub.*, 2006, **150**, 13–23; (*b*) A. Caruso, J. C. Lancelot, H. El-Kashef, M. S. Sinicropi, R. Legay, A. Lesnard and S. Rault, *Tetrahedron*, 2009, **65**, 10400; (*c*) A. Caruso, A. S. Voisin-Chiret, J. C. Lancelot, M. S. Sinicropi, A. Garofalo and S. Rault, *Molecules*, 2008, **13**, 1312–1320.
14 (*a*) A. Caruso, A. Chimento, H. El-Kashef, J. C. Lancelot, A. Panno, V. Pezzi, C. Saturnino, M. S. Sinicropi, R. Sirianni and S. Rault, *J. Enzyme Inhib. Med. Chem.*, 2012, **27**, 609–613; (*b*) A. Caruso, A. S. Voisin-Chiret, J. C. Lancelot, M. S. Sinicropi, A. Garofalo and S. Rault, *Heterocycles*, 2007, **71**, 2203–2210.
15 F. Puoci, F. Iemma, R. Muzzalupo, U. G. Spizzirri, S. Trombino, R. Cassano and N. Picci, *Macromol. Biosci.*, 2004, **4**, 22–26.
16 C. Yang, G. Wang, Z. Lu, J. Sun, J. Zhuang and W. Yang, *J. Mater. Chem.*, 2005, **15**, 4252–4257.
17 O. I. Parisi, G. Cirillo, M. Curcio, F. Puoci, F. Iemma, U. G. Spizzirri and N. Picci, *J. Polym. Res.*, 2010, **17**, 355–362.
18 M. Lanzino, P. Maris, R. Sirianni, I. Barone, I. Casaburi, A. Chimento, C. Giordano, C. Morelli, D. Sisci, P. Rizza, D. Bono-filgio, S. Catalano and S. Andò, *Cell Death Dis.*, 2013, **4**, e724.
19 K. Li and H. D. H. Stover, *J. Polym. Sci., Polym. Chem. Ed.*, 1993, **31**, 3257–3263.
20 G. L. Li, H. Möhwald and D. G. Shchukin, *Chem. Soc. Rev.*, 2013, **42**, 3628–3646.
21 F. Puoci, F. Iemma, R. Muzzalupo, U. G. Spizzirri, S. Trombino, R. Cassano and N. Picci, *Macromol. Biosci.*, 2004, **4**, 22–26.
22 S. E. Shim, S. H. Yang, H. H. Choi and S. Choe, *J. Polym. Sci., Polym. Chem. Ed.*, 2004, **42**, 835–845.
23 A. Rechichi, C. Cristallini, U. Vitale, G. Ciardelli, N. Barbani, G. Vozzi and P. Giusti, *J. Cell. Mol. Med.*, 2007, **11**, 1367–1376.
24 Y. Hoshino, H. Koide, T. Urakami, H. Kanazawa, T. Kodama, N. Oku and K. J. Shea, *J. Am. Chem. Soc.*, 2010, **132**, 6644–6645.